NJC

Accepted Manuscript

This article can be cited before page numbers have been issued, to do this please use: C. Liu, Z. Zhang, X. Zhai, X. Wang, J. Gui, C. Zhang, Y. Zhu and Y. Li, *New J. Chem.*, 2019, DOI: 10.1039/C8NJ05815F.

ROYAL SOCIETY OF CHEMISTRY

rsc.li/njc

View Article Online
DOI: 10.1039/C8NJ05815F

Synergistic effect between copper and different metal oxides in the selective hydrogenolysis of glucose

Chengwei Liu[1], Zhaonan Zhang[1], Xuefeng Zhai[1], Xianzhou Wang[2,3], Jianzhou Gui[1,4]*, Chenghua Zhang[2,5]*, Yulei Zhu[2,5], and Yongwang Li[2,5]

[1] State Key Laboratory of Separation Membranes & Membrane Processes, College of Environment and Chemical Engineering, Tianjin Polytechnic University, Tianjin 300387, China

[2] State Key Laboratory of Coal Conversion, Institute of Coal Chemistry, Chinese Academy of Sciences, Taiyuan 030001, People's Republic of China

[3] University of Chinese Academy of Sciences, Beijing 100049, People's Republic of China

[4] School of Material Science and Engineering, Tianjin Polytechnic University, Tianjin 300387, China

[5] National Energy Center for Coal to Liquids, Synfuels China Technology Co., Ltd., Huairou District, Beijing 101407, People's Republic of China

*Corresponding authors

E-mail address: jzgui@hotmail.com. Tel.: +86-22-83955668 (J. Gui).

E-mail address: zhangchh@sxicc.ac.cn. Tel.: +86-10-69667802 (C. Zhang).

View Article Online
DOI: 10.1039/C8NJ05815F

Abstract

Copper catalysts had been extensively applied in saccharide hydrogenolysis for their high selectivity to C-O bond cleavage. The hydrogenolysis of glucose contains many reaction procedures, which needs the synergistic effect of different active sites. A series of Cu catalysts supported on metal oxides with different surface physicochemical properties were prepared. The metal oxide supports not only influence the properties of Cu such as dispersion and electronic state, but also affect the activity of C-C and C-O bond cleavage in glucose. Furthermore, the coordination of a large amount of Lewis acid sites and hydrogenation sites on Cu/γ-Al_2O_3 catalyst can promote the C-C and C-O bond cleavage, leading to the selective conversion of glucose to glycol (selectivity of 66.6%). The Cu/MgO catalyst with a large amount of basic sites and metal sites could accelerate the retro-aldol condensation and isomerization reactions simultaneously, resulting the main products of C_2, C_3, and C_4 polyols. The study of the synergistic effect between other transition metals and γ-Al_2O_3 showed that Pd had high activity for the central C-C bond cleavage in glucose. Ru provided an extremely strong activity for the C-C bond cleavage at the terminal of the carbon chain in glucose, with the main product of methane (selectivity of 66.4%).

Keywords: glucose, hydrogenolysis, glycol, copper, acid/basic sites

View Article Online
DOI: 10.1039/C8NJ05815F

1. Introduction

The depletion of the non-renewable fossil fuel resources, combined with the ongoing climate change, indicates the necessity of the shift of the feedstock base towards sustainable biorefinery approach.[1-5] Since cellulose is the most abundant renewable resource in nature and may not compete with the production of edible crops, the efficient conversion of cellulose and its derivatives has attracted much attention. D-glucose, as the only monomer of cellulose, is a particularly simple and promising platform molecule of biomass for better understanding the complex process occurring in the conversion of polysaccharides.[6] Therefore, the catalytic conversion of glucose plays an important role in the production of a variety of valuable chemicals in the utilization of biomass resources. Furthermore, significant efforts have been devoted to the transformation of glucose by various catalytic processes involving hydrogenation, hydrogenolysis, dehydration, isomerization, oxidation and so on.[7-11] In this respect, the hydrogenation/hydrogenolysis of saccharides and polyols, by selectively breaking C-C and C-O bonds, provides an efficient and environmental benign process for the catalytic conversion of glucose to value-added chemicals and liquid hydrocarbons such as sorbitol, glycerol, propanediol (PDO), ethylene glycol (EG), hexane, etc.[12-14]

Copper catalysts were often used for sugar hydrogenolysis at 235-250 ^{o}C.[15,16] They were found to be excellent alternatives for sugar and sugar alcohol hydrogenolysis due to their relatively low activity for the hydrogenolysis of C-C bonds and high efficiency for C-O bond cleavage.[17,18] For example, the copper chromium oxide catalyst has been used by Zartman and Alkins for the hydrogenolysis of glucose in supercritical ethanol,[19]

View Article Online
DOI: 10.1039/C8NJ05815F

with 60% yield of 1,2-PDO. Furthermore, copper catalysts were often selected for the hydrogenolysis of glycerol and sorbitol to PDO (1,2-PDO and 1,3-PDO).[18,20,21] Typically, Chaminand obtained nearly 100% selectivity of 1,2-PDO at a low glycerol conversion on a Cu-ZnO catalyst.[22] Guo[20] tested a series of Cu/γ-Al_2O_3 catalysts with different amounts of copper, with 96.8% selectivity and 49.6% conversion achieved at 493 K and 1.5 MPa H_2 pressure. However, the coordination of copper and acid/basic sites has not been studied systematically.

With respect to the former researches on glucose hydrogenolysis, many disadvantages also exist which prevent the selective conversion of the promising feedstocks. Alkali additives such as NaOH and $Ca(OH)_2$ had often been used to promote the C-C cleavage activity.[23,24] However, the alkali existing in the reaction solution could cause the excessive degradation and product separation problem.[25] Obviously, many other drawbacks, such as the low selectivity, harsh conditions and environmental pollution also inhibit the effective conversion of glucose. In order to develop an economical and environmental benign process for glucose conversion, heterogeneous catalytic system was selected in this text.

As widely accepted that the bifunctional catalysts containing metal sites and acid/basic sites are most efficient for the hydrogenolysis of glucose, with the synergistic effect of different active sites. Furthermore, the elemental reactions of saccharide hydrogenolysis, occurring at the hydrogenation conditions with metal catalysts, mainly contain hydrogenation/dehydrogenation, isomerization, retro-aldol/aldol condensation, and dehydration reactions.[1,2] The hydrogenation and dehydrogenation reactions are

View Article Online
DOI: 10.1039/C8NJ05815F

conducted on the transition metal sites. The retro-aldol condensation reaction that leads to the cleavage of C-C bonds occurs on metal sites. The C-O bond cleavage of polyols can be catalyzed by the acid sites through dehydration.[1,26] However, the transition metal sites could also catalyze the cleavage of C-C/C-O bonds through the direct hydrogenolysis reaction, which makes the reaction more complicated.[23,24] For glucose transformation, the basic sites and the Lewis acid sites are also responsible for the isomerization between glucose and fructose. Based on the reaction pathway, the synergistic effect between metal and metal oxides with different acid/basic sites plays an important role in the product selectivity. For example, Wang studied the hydrogenolysis of sorbitol over MgO-supported Ni, Cu, and Co catalysts.[25,27] C_2 and C_3 polyols such as glycerol, 1,2-PDO, and EG were the main products. Huang et al. have compared the activity and selectivity of Cu supported on SiO_2, Al_2O_3 MgO, ZrO_2, CeO_2, and ZnO for xylitol hydrogenolysis.[28] Cu-SiO_2 showed the highest selectivity for EG and PDO among the prepared catalysts. However, the coordination effects between copper and different metal oxides in the bifunctional catalysts for the selective conversion of glucose have not been studied yet.

In this article, a series of metal oxides with different surface acid/basic properties were selected for copper catalysts. The relationships between the physicochemical properties and catalytic performance of copper catalysts were studied in detail. Furthermore, the synergistic effects between γ-Al_2O_3 and different transition metals were also studied.

2. Material and Methods

View Article Online
DOI: 10.1039/C8NJ05815F

2.1. Catalysts preparation

ZrO_2 and TiO_2 were purchased from Nanjing Haitai nanometer material Co., Ltd. γ-Al_2O_3 was from sinopharm chemical reagent Co., Ltd. MgO was prepared by a co-precipitation method using the 0.5 M magnesium nitrate aqueous solution and 0.5 M ammonia at pH 9. The precipitate was aged for 1 h, then separated with filtration and washed with deionized water until the filtrate was neutral. Then the precursor was dried at 120 ^{o}C overnight and calcined at 500 ^{o}C for 5 h. SiO_2 was prepared by colloidal silica aqueous solution (SiO_2, 30 wt%, Qingdao, Ocean Chemical Co., Ltd., China) dehydration at 60 ^{o}C followed by dried at 120 ^{o}C and calcined at 500 ^{o}C for 5 h. All the metal oxide supports were granted into size 20-40 mesh before used.

All the catalysts were prepared by an incipient wetness impregnation method. The contents of Cu and Ni were designed as 5 wt%, and Pd and Ru were 2 wt%. Take Cu/γ-Al_2O_3 for example, 10 g γ-Al_2O_3 was impregnated with 13 mL copper nitrate aqueous solution containing 1.9 g $Cu(NO_3)_2 \cdot 3H_2O$. After impregnation, the sample was dried at 120 ^{o}C overnight and then calcined at 500 ^{o}C for 5 h.

2.2 Catalysts characterization

ICP optical emission spectroscopy (Optima2100DV, PerkinEler) was performed to measure the copper loading of the calcined copper catalysts.

The BET surface area of the calcined catalysts was measured on a micromeritics ASAP 2420 instrument. All the samples were degassed at 110 ^{o}C for 1 h and 350 ^{o}C for 8 h before the measurement.

Powder X ray diffraction (XRD) patterns were obtained on a D/max-RA X-ray

View Article Online
DOI: 10.1039/C8NJ05815F

diffractometer (Bruker, Germany), with Cu-Kα radiation operating at 30 KV and 100 mA. The XRD patterns were recorded in 2θ values ranging from 10° to 80°.

DRIFTS spectra of CO adsorption were collected using an infrared spectrometer (VERTEX70, Bruker, Germany). The infrared cell with ZnSe windows was connected to a gas-feed system, which allowed the in situ measurement of the adsorption of CO. Prior to measurement, the catalysts were reduced in situ at 250 °C for 10 h in H_2 flow (20 mL/min). The sample was flushed with helium for 1 h at 250 °C. Then the system was cooled to 30 °C in helium flow for the CO-FTIR record.

NH_3 temperature-programmed desorption (NH_3-TPD) measurements and CO_2 temperature-programmed desorption (CO_2-TPD) measurements were conducted on an AutoChem II 2920 equipment (Mircromeritics, USA). In a typical run, 200 mg catalyst was put into a u-shaped quartz tube. The sample was first pretreated in a helium flow at 500 °C for 1 h. After cooling to 100 °C in the helium flow, the sample was adsorbed with NH_3 or CO_2 until saturation, then flushed with helium for 1 h to remove the physical adsorption. The NH_3 or CO_2 desorption pattern was recorded using MS detectors from 100 °C to 500 °C at a heating rate of 10 °C/min.

The Py-FTIR spectra were obtained using a VERTEX70 Bruker FT-IR spectrometer. All the samples were pretreated by degassing to a pressure of 10^{-2} MPa at 350 °C for 1 h. The Py-FTIR spectra were measured at 30 °C after evacuations at 30 °C, 200 °C, and 350 °C for 30 min.

Adsorptive decomposition of N_2O was conducted using the method reported previously.[29-31] The exposed copper surface area was calculated based on the assuming

View Article Online
DOI: 10.1039/C8NJ05815F

spherical shape of the copper metal particles and 1.4×10^{19} copper atoms/m^2. For one measurement, the catalyst was reduced at 350 °C in a 10 vol% H_2/Ar flow for 15 min firstly. Then it was exposed to N_2O at 40 °C for 30 min. Finally, the H_2-TPR was recorded with the 10 vol% H_2/Ar flow after flushing with Ar (50 mL/min) for 30 min.

2.3. Catalytic reaction process

The catalytic tests were carried out in a tubular fixed-bed reactor (i.d. 12 mm, length 600 mm). For a typical run, 6 mL catalysts were packed at the flat-temperature zone and in situ reduced at 250 °C for 10 h with a stream of pure hydrogen. The reactant was introduced into the reactor with an HPLC pump along with a co-feed H_2 of gas flowing. The liquid products collected in the cold trap were analyzed by a high performance liquid chromatograph (HPLC) equipped with an RID detector. The gas products were analyzed in situ by gas chromatograph (GC) (models 6890N and 4890D; Agilent). Typical reaction conditions are as follows: 180 °C, 4 MPa H_2, 5 wt% glucose (sorbitol, fructose, glycerol) aqueous solution, ratio of H_2 to glucose = 161:1 (molar ratio), LHSV = 0.2 h^{-1}.

The total carbon (TC) balance was also measured. TC in feedstock and liquid products after reaction was detected by German elementar (Vario EL cube). Sulfanilamide was used as a standard sample which contains 41.81% of C. The carbon content in gas was calculated from concentration values obtained by GC chromatographic analysis. Then TC was calculated by the following equation:

$$\mathrm{TC}(\%) = \frac{\text{Carbon in liquid product} + \text{Carbon in gas product}}{\text{Carbon in feedstock}} \times 100$$

The conversion of glucose and the selectivity of products were quantified by the

View Article Online
DOI: 10.1039/C8NJ05815F

following equation:

$$\text{Conversion (\%)} = 100 - \frac{\text{carbon mol of reactant after reaction}}{\text{carbon mol of reactant in feedstock}} \times 100$$

$$\text{Selectivity (\%)} = \frac{\text{carbon mol of each product}}{\text{sum of carbon mol for all products}} \times 100$$

3. Results and discussion

3.1. Physicochemical properties of the prepared catalysts

Table 1. Physicochemical properties of the prepared catalysts

Catalyst	Cu (mmol/gCat)[a]	S_{BET} (m^2/g)[b]	S_{Cu} (m^2/g)[c]	Acidity (μmol/g)[d]	Basicity (μmol/g)[e]
Cu/SiO_2	0.71	171.4	0.5	21.7	23.9
$Cu/\gamma\text{-}Al_2O_3$	0.73	171.1	44.8	88.8	40.0
Cu/MgO	0.73	53.0	11.2	16.7	45.0
Cu/TiO_2	0.72	23.9	3.0	29.6	23.5
Cu/ZrO_2	0.73	20.4	8.0	23.1	26.1

[a] ICP method. [b] BET method. [c] Copper metal surface area, determined by the N_2O-decomposition method. [d] Measured by NH_3-TPD. [e] Measured by CO_2-TPD.

The supports such as γ-Al_2O_3, MgO, ZrO_2, TiO_2, and SiO_2 with special surface properties were tested. γ-Al_2O_3, with the large amount of acid sites, is extensively used in industrial processes.[32] The amphoteric properties of ZrO_2 and TiO_2 are favorable for saccharide conversion which needs the synergetic catalysis of different active sites.[33] MgO also plays a good performance on polyols conversion to glycerol and glycol.[25] SiO_2 has been widely researched for glycerol conversion, with a high selectivity of PDO obtained.[34]

The physicochemical properties of the copper-based catalysts are listed in Table 1. The small discrepancy of Cu loadings could be due to the loss in preparation procedure. The surface areas of the calcined copper catalysts decreased with the order: Cu/SiO_2 ~

View Article Online
DOI: 10.1039/C8NJ05815F

Cu/γ-Al_2O_3 > Cu/MgO > Cu/TiO_2 > Cu/ZrO_2.

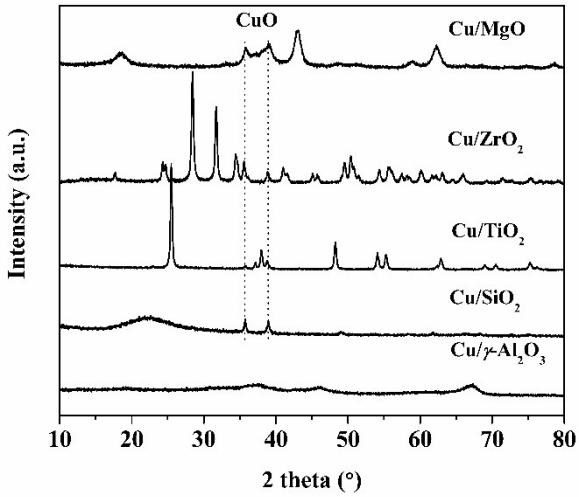

Figure 1. XRD patterns of the calcined catalysts.

The X ray diffraction patterns were obtained to detect the dispersion of copper (Figure 1). Most of the catalysts showed the CuO peaks at 2θ = 35.5° and 38.7° (JCPDS 48-1548) except Cu/γ-Al_2O_3. It indicates that CuO particles were dispersed very well on the large surface of γ-Al_2O_3. The N_2O adsorptive decomposition method is reliable to character the copper surface area. The results showed that Cu/γ-Al_2O_3 had the highest copper surface area (44.8 m^2/g), which was consistent with the XRD results. However, copper surface areas showed a great discrepancy with the catalyst surface areas, which suggested that the copper surface area not only depended on the physical dispersion of the supports, but also had correlation with the metal-support interaction. The lowest dispersion of Cu on SiO_2 depends strongly on the preparation method of the catalysts, which can cause the weak metal-support interaction.[35] For example, the high calcination of SiO_2 and the catalyst precursor could decrease the surface silanol concentration, which is disadvantage to the dispersion of copper nanoparticles.[36,37] The dispersion of copper on different supports decreased with the following order: Cu/γ-Al_2O_3 >

View Article Online
DOI: 10.1039/C8NJ05815F

Cu/MgO > Cu/ZrO_2 > Cu/TiO_2 > Cu/SiO_2.

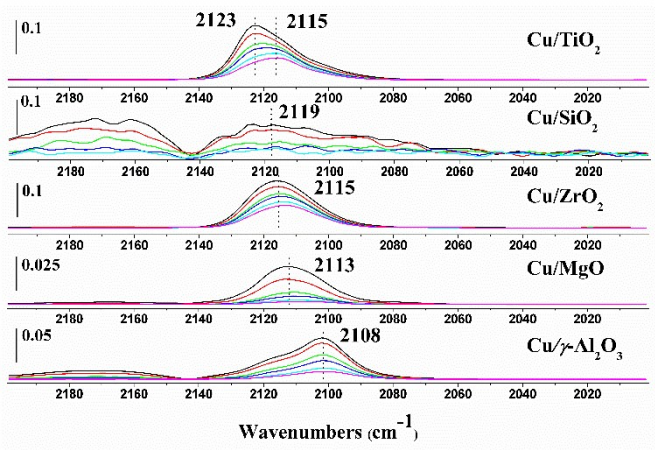

Figure 2. CO-DRIFT patterns of the reduced catalysts.

CO is used as a probe molecule to study the metal-support interaction, as shown in Figure 2. The bands of CO adsorption on the reduced catalysts changed along with the chemical environment of the metal. Generally, the bands at 2110 cm^{-1} and below are ascribed to CO on zero-valent copper metal particles. The bands between 2110 cm^{-1} and 2135 cm^{-1} are assigned to CO irreversibly adsorbed on cuprous ions.[38] The pattern of Cu/TiO_2 shows a broad band with the peak at 2123 cm^{-1} after purging helium for half a minute, which shifted to a lower band at 2115 cm^{-1} after purging helium for 15 min. This indicates that there are at least two different sites on the Cu/TiO_2 surface. Therefore, it's reasonable to spite the band into two peaks at 2123 cm^{-1} and 2115 cm^{-1}. The band at 2115 cm^{-1} is ascribed to CO adsorbed on imperfect sites, such as step and edge sites. The band at 2123 cm^{-1} could be assigned to CO adsorbed on isolated Cu atoms and/or small 2D Cu particles on the TiO_2 surface. Small 2D Cu particles in Cu/TiO_2 are partially electropositive as a result of interactions with oxygen atoms on the surface of the support, as reported by Boccuzzi et al.[39,40] The Cu/SiO_2 catalyst showed the band at

View Article Online
DOI: 10.1039/C8NJ05815F

2119 cm^{-1}, which was easily removed after purging helium for a short time. Ferullo and Castellani have assigned this band to CO adsorbed on electropositive copper linked to a Si-O* site when the peak is reversible.[41] The band of CO adsorbed on Cu/ZrO_2 was stable at 2115 cm^{-1}, which could be ascribed to CO adsorbed on Cu^+ sites.[42] The bands of CO adsorbed on Cu/MgO and Cu/γ-Al_2O_3 were at 2110 cm^{-1} and 2113 cm^{-1}, which almost disappeared after purging helium for 15 min. It is suggested that the bands could be assigned to CO-Cu^0 sites.[38,43] Therefore, as a result of the interaction between metal oxides and copper, copper species with different valences existed on the catalyst surface. In summary, CuO was easily reduced on MgO and γ-Al_2O_3, resulting in the main species of Cu^0 on the catalyst surface. CuO was difficult to be reduced on TiO_2 and ZrO_2, which could be due to the strong interaction between Cu and the metal oxides. CuO was also not easy to be reduced on the SiO_2 support, which is due to the large particle size of CuO.

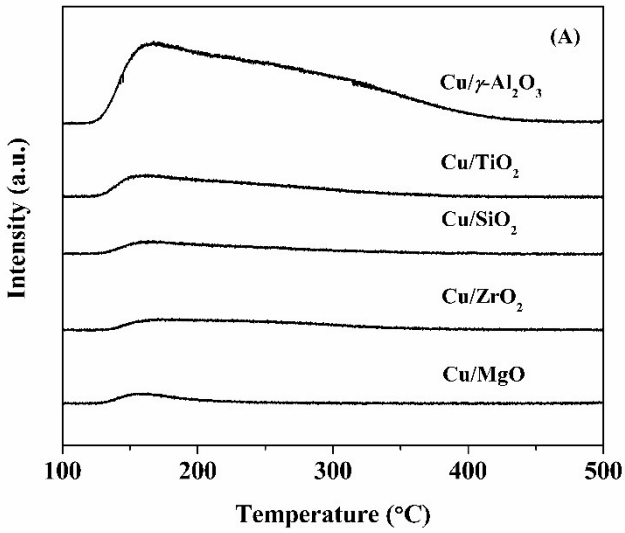

View Article Online
DOI: 10.1039/C8NJ05815F

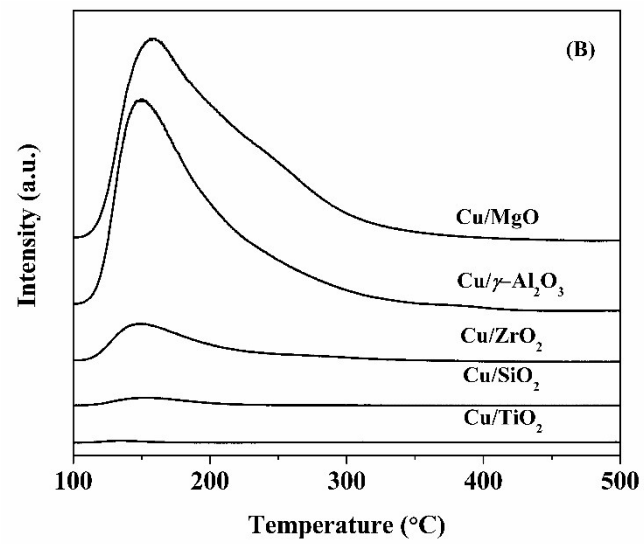

Figure 3. NH_3-TPD (A) and CO_2-TPD (B) patterns of the calcined copper catalysts.

NH_3-TPD and CO_2-TPD were performed to identify the acidity and basicity of the catalysts respectively. The amounts of acid and basic sites, as listed in Table 1, were calculated by the integrating curves and calibrated by standard NH_3 and CO_2 gases. The amounts of acid sites on the catalyst surface decreased in the following order: Cu/γ-Al_2O_3 > Cu/TiO_2 > Cu/ZrO_2 > Cu/SiO_2 > Cu/MgO (Table 1). As shown in Figure 3A, Cu/γ-Al_2O_3 had a main peak at 172 ^oC with a shoulder peak at around 258 ^oC, indicating that there were weak and medium acid sites on the surface of Cu/γ-Al_2O_3. In the case of Cu/TiO_2, Cu/ZrO_2, Cu/SiO_2, and Cu/MgO catalysts, only one peak at about 150 ^oC was observed, which can be ascribed to the weak acid sites. The amounts of the basic sites in the copper catalysts decreased with the following order: Cu/MgO > Cu/γ-Al_2O_3 > Cu/ZrO_2 > Cu/SiO_2 ~ Cu/TiO_2. Figure 3B shows the CO_2-TPD profiles of the copper catalysts. For the Cu/γ-Al_2O_3, Cu/ZrO_2, Cu/SiO_2, and Cu/TiO_2 catalysts, only a broad peak at 150 ^oC was observed, which is corresponding to the weak basic sites on the

View Article Online
DOI: 10.1039/C8NJ05815F

catalysts surface. However, a new shoulder peak at about 212 °C was observed on Cu/MgO, which could be attributed to the medium basic sites on the catalyst surface. The results indicate that there were large amounts of weak and medium acid sites and weak basic sites on the surface of the Cu/γ-Al_2O_3 catalysts, with the acid/basic sites mol ratio of 2.2. The surface properties of γ-Al_2O_3 are changeable with the processing method. For example, the calcination process could cause the remove of the hydroxyl group on γ-Al_2O_3 surface, which could bring new Lewis acid sites by the electron deficient aluminium ions. Many researchers have also detected the surface acid and base properties using CO_2-TPD and NH_3-TPD.[44-47] For example, Kumar et al. performed the CO_2-TPD and NH_3-TPD of two kinds of commercial Al_2O_3.[47] The results turned out that one Al_2O_3 sample showed nearly the same desorption amounts of CO_2 and NH_3, with the values of 56.6 μmol g^{-1} and 55.6 μmol g^{-1}, respectively. Both the Cu/ZrO_2 and Cu/TiO_2 catalysts had small amounts of acid and basic sites on the catalyst surface. Relatively low amounts of acid and basic sites are present on the Cu/SiO_2 catalysts surface. The Cu/MgO catalyst displayed the largest amounts of weak and medium basic sites and the lowest amount of acid sites.

Py-FTIR spectra were obtained to identify the nature of acid sites on the different supported catalysts, as illustrated in Figure 4. For the spectra of pyridine adsorbed on Cu/γ-Al_2O_3 when outgassing at 30 °C, the bands at 1577 cm^{-1} and 1593 cm^{-1} represent physically adsorbed pyridine and hydrogen-bonded pyridine respectively,[48] considering their disappearance after evacuation at higher temperature. The band at 1448 cm^{-1}, 1489 cm^{-1}, and 1610 cm^{-1} were ascribed to the coordination of Py molecules to Lewis acid

View Article Online
DOI: 10.1039/C8NJ05815F

sites and consequent formation of LPy species. Moreover, the decrease of the intensity and the increase in the frequency of the peak after evacuation at subsequent higher temperatures obviously indicated that there were both weak and medium Lewis acid sites on the surface of Cu/γ-Al_2O_3.[1,49,50] The bands around 1445, 1489, 1574, and 1604 cm^{-1} in the spectrum of Cu/TiO_2 and Cu/ZrO_2 at 30 °C showed the strong features of the formation of LPy species.[49] However, the peak of the LPy species was very weak and almost disappeared after evacuation at 200 ºC, suggesting that there were only small amounts of weak Lewis acid sites on the surface of Cu/TiO_2 and Cu/ZrO_2. The peak of pyridine adsorbed on Cu/SiO_2 at 30 ºC dramatically decreased at 200 ºC, which indicated there was only weak acid sites on the catalyst surface. The bands at 1439, 1485, and 1597 cm^{-1} in the spectrum of the Cu/MgO catalyst after evacuation at 30 ºC represent hydrogen-bonded pyridine. The peaks totally disappeared as expected.

In this context, only a weak shoulder band at around 1540 cm^{-1} was found for the Cu/γ-Al_2O_3 catalyst. The results were consistent with Chen's report, which also showed that only a negligible amount of Brønsted acid existed on the Al_2O_3 surface.[51] However, no band at 1540 cm^{-1} was found for the other catalysts, indicating the absence of Brønsted acid sites. For the Cu/γ-Al_2O_3 catalyst, there were weak and medium Lewis acid sites. There were only weak Lewis acid sites on the surface of Cu/SiO_2, Cu/TiO_2, and Cu/ZrO_2 catalysts. The Cu/MgO catalyst was lack of acid sites. These were consistent with the NH_3-TPD results.

View Article Online
DOI: 10.1039/C8NJ05815F

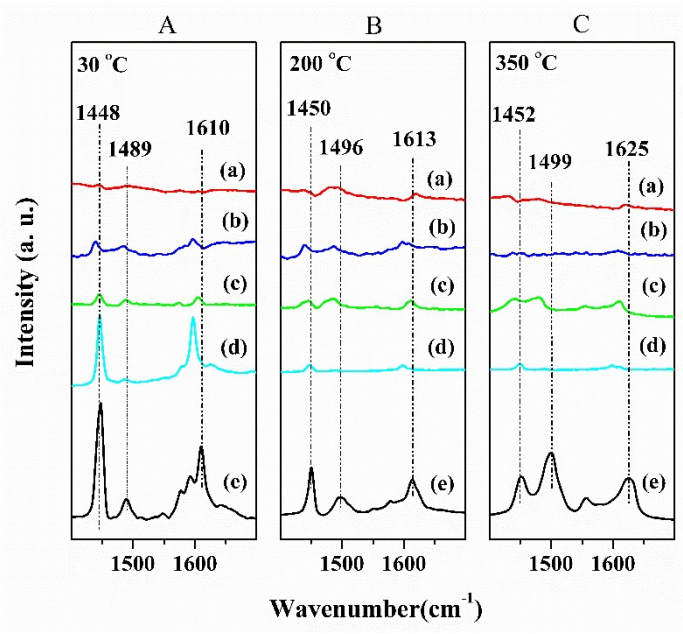

Figure 4. Py-FTIR spectra of the calcined catalysts after adsorption of pyridine and subsequent evacuation at different temperatures for 30 min: (a) Cu/ZrO_2, (b) Cu/MgO, (c) Cu/TiO_2, (d) Cu/SiO_2, (e) $Cu/\gamma\text{-}Al_2O_3$.

3.2. The catalytic performance of copper-based catalysts in glucose hydrogenolysis

The results of glucose hydrogenolysis over different supported Cu catalysts were shown in Table 2. Significant efforts had been devoted to the qualitative/quantitative measurements of the product distributions using the HPLC and GC/GC-MS methods. Glucose was almost totally converted over the prepared catalysts. CO_2, CH_4 or other carbon containing gas products were not detected in the tail gas. The products in liquid phase mainly included sorbitol, glycerol, EG, and PDO. Small amounts of other products such as methanol, ethanol, propanol, butanol, 1,2-butanediol, 1,4-butanediol, erythritol, and xylitol were also detected in the liquid phase. Soluble polymeric byproducts were detected in the liquid after reaction. The carbon balance was generally better than 88% over most of the catalysts except Cu/TiO_2, with only 28.8%. Most of

View Article Online
DOI: 10.1039/C8NJ05815F

the glucose feedstock was transformed into insoluble humins.

Cu/γ-Al_2O_3 showed high selectivity for EG and PDO, with a combined selectivity of 66.6% (8.6% for EG and 58.0% for PDO) at 99.4% conversion of glucose. Including glycerol, the selectivity to the sum of these polyols (EG, PDO, and glycerol) reached 77.7%, which was much higher than those on the other supported catalysts. Cu/MgO and Cu/ZrO_2 also showed relatively high glycol selectivity (55.0% and 40.0% respectively). However, it is interesting to note that, the selectivity of EG and glycerol on Cu/MgO, with 14.0% and 20.0% respectively, was higher than those on other catalysts. The total selectivity of these polyols (EG, PDO, and glycerol) on Cu/TiO_2 catalysts was only 4.2%. Furthermore, the aqueous soluble polymers were the major products in the liquid. The results of Cu/SiO_2 showed that the hydrogenation reaction was dominating, leading to the highest sorbitol selectivity of 82.4%. In contrast, only a small amount of the lower hydrogenolysis products were present in the liquid. The selectivity of glycol was only 5.0%.

The catalytic conversion of glucose to the desired product needs the selective cleavage of C-C and C-O bonds. Therefore, the integral C-C and C-O bond cleavage ratios were summarized in Table 2. By assuming that the soluble polymer and the insoluble humins were regarded as the products with no C-C and C-O bond cleavage, the detail definition is as follows:

$$\mathrm{C-O}\ (\%) = \left(1 - \frac{\text{C–O bond mol of product}}{\text{C–O bond mol of converted glucoses}}\right) \times 100 \qquad (1)$$

$$\mathrm{C-C}\ (\%) = \left(1 - \frac{\text{C–C bond mol of product}}{\text{C–C bond mol of converted glucoses}}\right) \times 100 \qquad (2)$$

Table 2. The activities and selectivities of glucose hydrogenolysis on the prepared catalysts[a]

Catalyst	Conv. (%)	Selectivity (on a carbon basis, %)						C_3 (mol%)	$C_2 + C_4$ (mol%)	C-C/C-O bond cleavage ratio (%)		TC (%)
		Sorbitol	EG	Glycerol	PDO	Glycol[b]	Others[c]			C-C	C-O	
Cu/γ-Al_2O_3	99.4	3.5	8.6	11.1	58.0	66.6	18.8	70.6	19.0	21.2	37.8	100
Cu/MgO	99.6	3.4	14.0	20.0	41.0	55.0	21.6	61.9	24.9	19.2	31.5	95.8
Cu/ZrO_2	99.2	7.0	5.4	9.5	34.6	40.0	43.5	47.6	22.7	14.5	32.1	80.3
Cu/SiO_2	96.3	82.4	0.5	1.4	4.5	5.0	11.2	6.2	5.8	6.3	18.3	100
Cu/TiO_2	97.2	0.9	0.5	0.5	3.2	3.7	94.9	5.7	5.4	13.8	8.8	28.8
Ni/γ-Al_2O_3	99.0	2.4	3.4	2.5	28.8	32.2	62.9	31.8	13.9	11.2	34.3	53.8
Pd/γ-Al_2O_3	99.4	2.5	6.4	4.3	50.4	56.8	36.4	62.8	43.3	24.7	43.6	100
Ru/γ-Al_2O_3	95.3	0.0	0.0	0.0	0.9	0.9	99.1[d]	9.1	10.9	70.2	84.5	92.6

[a] Reaction condition: 5 wt% glucose aqueous solution, 4 MPa, 180 °C, H_2-glucose = 161:1 (mol ratio), and LHSV = 0.2 h^{-1}. [b] EG and PDO. [c] Others include xylitol, erythritol, 1,2-butanediol, methanol, ethanol, propanol, butanol, etc. [d] Include 84.6% selectivity of alkanes from C_1 to C_6, with 66.4% methane.

View Article Online
DOI: 10.1039/C8NJ05815F

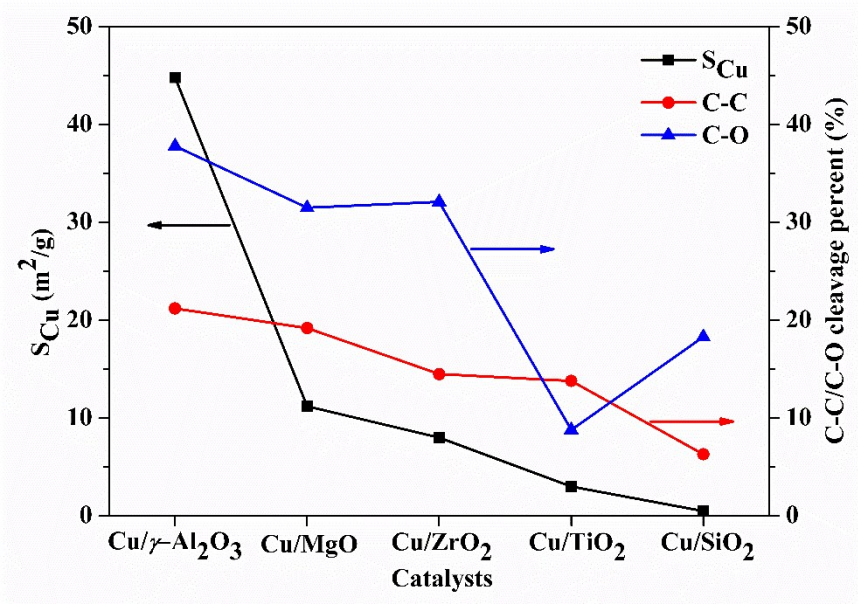

Figure 5. The correlation between Cu surface area and the C-C/C-O bond cleavage percent.

The results of C-C and C-O bond cleavage ratios of glucose showed that there was even no cleavage of C-O and C-C bonds occurring on Cu/SiO_2. The highest selectivity of sorbitol is considered to be related with the nearly neutral surface of the catalyst and the agglomerated Cu particles, which provide weak dehydration and retro-aldol condensation reaction activity. In contrast, Cu/TiO_2 showed very low copper surface area and hydrogenation activity, resulting in the main products of soluble and insoluble polymer after reaction. Cu/γ-Al_2O_3, with the highest copper surface area and acid amounts, showed the highest C-O and C-C bond cleavage activity. It suggests that the coordination of acid/basic sites and the copper sites could not only promote the cleavage of C-C/C-O bonds but also the efficient hydrogenation of the intermediate fragments. The correlation between Cu surface area and the C-C/C-O bond cleavage percent has been drawn and provided in Figure 5. The results showed that the C-C bond cleavage percent of glucose displayed a similar decrease tendency with the decreasing of Cu

View Article Online
DOI: 10.1039/C8NJ05815F

surface areas of the supported Cu catalysts. It indicates that the dispersion of Cu played a significant role in C-C bond cleavage. However, it is known that Cu has lower activity for C-C bond cleavage through the straightforward hydrogenolysis. Furthermore, many researchers have also conducted the retro-aldol condensation reaction on metal catalysts, indicating that the metallic sites are the active site.[13,26,52,53] Accordingly, the retro-aldol condensation reaction can be performed at acid, basic or even neutral conditions. For example, Torresi has studied the conversion of diols on copper-silica catalysts. They pointed out that retro aldol-like reactions occurred on metallic Cu sites.[53] Considering the carbon balance and the Cu active sites for the retro-aldol condensation reaction, it suggests that the well dispersed Cu sites could not only inhibit the polymerization of glucose and the unsaturated intermediates by promoting their hydrogenation/dehydrogenation reactions, but also promote the retro-aldol condensation reaction efficiently. The retro-aldol condensation mechanism of the hydrogenolytic cleavage of polyols was proposed in the 1980s by the group of Montassier, which has been widely accepted.[1,54-56] They postulated that C-C bond cleavage of polyols was catalyzed by adsorbed hydroxyl species on the metal catalyst surface. Therefore, we speculated that Cu could promote the retro-aldol condensation reaction by the adsorbed hydroxyl groups on the Cu^0 sites. However, the variation trend of the percent of C-O bond cleavage was not strictly followed that of Cu surface area. The discrepancy could be due to the effect of acidic sites on the catalyst surface. The overall C_3 and $C_2 + C_4$ product selectivities were also summarized. Cu/γ-Al_2O_3 showed the highest C_3 product selectivity. It is related with the promoting effect of Lewis acid

View Article Online
DOI: 10.1039/C8NJ05815F

on the isomerization, which were the intermediate reaction procedures of the hydrogenolysis of glucose to C_3 product. Moreover, Cu/MgO showed the highest C_2 + C_4 product selectivity compared with other catalysts.

3.3. The effect of different transition metals in glucose conversion

The above text showed that the hydrogenation activity played an important role on the product selectivity. Furthermore, the transition metal also has the direct hydrogenolysis activity towards the C-C/C-O bonds, which will make the reactions and products of glucose hydrogenolysis more complicated. For example, Ru and Pt supported on activated carbon were used for glucose hydrogenolysis at 180 ºC.[57] The Pt/AC catalysts displayed high selectivity toward sorbitol. On the other hand, the Ru/AC catalysts showed higher selectivity toward C_3-C_6 polyols, with sorbitol selectivity of only 55-90%. Therefore, the coordination effect between γ-Al_2O_3 and different transition metals with various hydrogenolysis activities have been studied. The hydrogenolysis of glucose over Ni/γ-Al_2O_3, Pd/γ-Al_2O_3, and Ru/γ-Al_2O_3 were compared. The product distribution over different metal catalysts varied widely. The glycol product selectivity was very low on Ni/γ-Al_2O_3. A considerable amount of xylitol, erythritol, and 1,2-butanediol existed in the liquid products. A small amount of methane was also detected in the gas phase. This result is similar with the report of Ye.[58] CH_4 was also formed in the hydrogenolysis of sorbitol on the Ni/γ-Al_2O_3 catalyst, with the selectivity of 8.3%. It displays that Ni has activity to break C-C bond at the terminal of the carbon chain of glucose, with the total C-C and C-O bond cleavage ratios of 11.2% and 34.3% respectively. Pd/γ-Al_2O_3 showed very high selectivity for PDO (50.4%). The

View Article Online
DOI: 10.1039/C8NJ05815F

total C-C and C-O bond cleavage ratios were 24.7% and 43.6% respectively, suggesting that Pd has high activity for the cleavage of the central C-C bonds of glucose. Ru/γ-Al_2O_3 had very low selectivity to polyols, with the total selectivity below 10%. In contrast, the alkane selectivity was up to 84.6%, with 66.4% selectivity of methane. It suggests that Ru has the highest activity for C-C and C-O bond cleavage, with the C-C and C-O bond cleavage ratios of 70.2% and 84.5% respectively. Furthermore, the C-C bond cleavage mainly occurs at the terminal of the carbon chain of glucose.[59]

3.4. The function of supports in glucose conversion

Table 3. The conversion of glucose on different supports[a]

Catalyst	Conversion (%)	Selectivity (%)						TC (%)
		Fructose	Glycerol	EG	PDO	HMF	Others[b]	
Blank	33.1	37.4	0.8	0.0	14.0	24.1	25.1	97.2
γ-Al_2O_3	90.8	2.8	0.0	0.8	2.8	4.3	89.3	33.0
ZrO_2	94.7	1.9	0.0	0.7	1.2	3.9	89.9	29.4

[a] Reaction condition: 5 wt% glucose aqueous solution, 4 MPa, 180 ^{o}C, H_2-glucose = 161:1 (mol ratio), LHSV = 0.2 h^{-1}. [b] Others include small amounts of methanol, ethanol, propanol, 1,2-butanediol, etc.

As mentioned above, the supports can provide not only a surface to disperse the active component, but also acid/basic sites to promote the isomerization, dehydration, and retro-aldol condensation reactions. In order to confirm the catalytic effect of the supports, two supports such as γ-Al_2O_3 and ZrO_2 with different acidity and basicity were tested. The results are displayed in Table 3. The conversion of glucose without

View Article Online
DOI: 10.1039/C8NJ05815F

any catalysts was only 33.1%. A certain amount of fructose and 5-hydroxymethylfurfural (HMF) were detected, with the selectivities of 37.4% and 24.1%, respectively. It suggested that the isomerization and dehydration reactions could be conducted in the hydrothermal condition without any catalyst in the H_2 atmosphere. These results are consistent with the report of Sasaki et al.[60] They conducted the transformation of glucose with none catalyst in supercritical water. Products from the retro-aldol condensation, isomerization, and dehydration reaction of glucose were obtained. When the catalytic transformation of glucose was conducted on γ-Al_2O_3 and ZrO_2, the conversion of glucose increased significantly. However, the selectivities of fructose, PDO, and HMF had decreased. Glucose was mainly converted to both insoluble humins and soluble polymeric byproducts. This could be attributed to the oligomerization reaction of glucose and/or the unsaturated intermediates, which can be carried out in the presence of an acid and basic catalyst through dehydration and aldol condensation.[61,62]

3.5. The catalytic conversion of Cu/γ-Al_2O_3 for other polyols

Table 4. The hydrogenolysis of different materials on Cu/γ-Al_2O_3[a]

Material	Conv. (%)	Selectivity (%)								TC
		Glucose	Sorbitol	Mannitol	Glycerol	EG	PDO	Glycol[b]	Others	(%)
Glucose	99.4	-	3.5	0.0	11.1	8.6	58.0	66.6	18.8	100
Fructose	100	1.0	0.0	5.3	9.4	5.3	47.2	52.5	31.8	81.6
Sorbitol	33.0	-	-	0	36.6	14.7	39.5	54.2	9.2	100
Glycerol	46.0	-	-	-	-	11.7	86.9	98.6	1.4	100

[a] Reaction condition: 5 wt% glucose aqueous solution, 4 MPa, 180 °C, H_2-glucose = 161:1 (mol ratio); LHSV = 0.2 h^{-1}. [b] EG and PDO

In order to study the synergistic effect of metal sites and the acid/basic sites on the intermediate products of glucose hydrogenolysis, the catalytic conversion of fructose,

View Article Online
DOI: 10.1039/C8NJ05815F

sorbitol, and glycerol were also performed on Cu/γ-Al_2O_3 at 180 ºC and 4 MPa. The results are displayed in Table 4. The product species of glucose and fructose hydrogenolysis were similar. All the products identified in glucose conversion were detected in fructose conversion. However, the carbon balance and the product selectivity were lower than that of glucose conversion. It suggested that humins was easier formed in fructose conversion than in glucose conversion. Glucose was also detected in the products of fructose conversion. It displayed that fructose could also isomerized to glucose in this reaction condition. Sorbitol was difficult to be degraded in the hydrogenation environment with Cu/γ-Al_2O_3 catalyst, with only 33.0% conversion obtained. Glycerol and glycol were the main products in the liquid phase, with the yields of 36.6 and 54.2% respectively. It has been identified that sorbitol was not the intermediate of producing glycerol and glycol in the hydrogenolysis of glucose.[63] Many reports also proved that the selective hydrogenation of glucose to sorbitol was the main undesirable competitive pathway for glycol producing.[64,65] The conversion of glycerol was similar with that of sorbitol (46.0%). Although the conversion was not very high, the selectivity of PDO reached 86.9%. Considering the hydrogenolysis performance of glucose and glycerol, PDO may be generated from the hydrogenolysis of glycerol or the intermediates of fructose conversion. Furthermore, it turned out that PDO was easier obtained from glucose than from glycerol in the reaction condition.

3.6. The synergistic effect between metal and metal oxide on the product distribution of glucose hydrogenolysis

View Article Online
DOI: 10.1039/C8NJ05815F

As illustrated above, the product distribution of glucose hydrogenolysis depended on the type and the relative catalytic activity of active sites. Only products from the dehydration and polymerization of glucose and the unsaturated intermediates were detected with only metal oxide catalysts. The neutral Cu/SiO_2 catalyst could mainly promote the hydrogenation of glucose to sorbitol. However, the synergistic effect between well dispersed Cu sites and the basic/Lewis acid sites could promote the hydrogenolysis of glucose to lower polyols. Furthermore, Lewis acid sites on γ-Al_2O_3 could promote the isomerization of glucose to fructose, which could be transformed to the C_3 product through retro-aldol condensation reaction on the well dispersed Cu sites. The unsaturated C_3 products then undergo the dehydration and hydrogenation reactions on Lewis acid sites and well dispersed Cu sites respectively, resulting the highest PDO selectivity on γ-Al_2O_3. Cu/MgO showed the highest C_2 selectivity compared with other catalysts. Furthermore, it has been suggested that glucose can be directly converted to C_2 and C_4 products through retro-aldol condensation.[60] It turned out that the Cu/MgO catalyst could accelerate the retro-aldol condensation and the isomerization reaction rates simultaneously, which is disadvantageous for the enhancement of product selectivity.

3.7. The role of support, Cu dispersion and Cu states

The NH_3-TPD and CO_2-TPD results showed that the oxide supports could provide Lewis acid and basic sites. Glucose and the unsaturated intermediates could form polymers on the acid and basic sites without efficient hydrogenation sites. However, in the hydrogen atmosphere, the basic sites could facilitate the isomerization and retro-

View Article Online
DOI: 10.1039/C8NJ05815F

aldol condensation reaction. Furthermore, the Lewis acid sites could promote the isomerization and dehydration reactions of glucose and the intermediates.

Liu et al. has studied the synergistic effect of Ru and WO_x on the bifunctional Ru-W/SiO_2 catalysts for the hydrogenolysis of glucose.[66] They suggested that the retro-aldol condensation reaction of glucose or fructose was conducted on WO_x acid sites. Pang et al. have performed the selective conversion of concentrated glucose to 1,2-propylene glycol and ethylene glycol on RuSn/AC catalysts.[67] They proposed that both RuSn alloy and the highly dispersed Sn^{4+} species could promote the retro-aldol condensation of glucose to form C_2 and C_3 intermediates. Holm and co-workers found that the Lewis acid sites on the zeotype catalysts, such as Ti-, Sn-, and Zr-Beta, could catalyze the retro aldol condensation reaction of the glucose and fructose.[68] Therefore, we proposed that the Lewis acid sites on the catalysts we prepared could also promote the retro-aldol condensation reaction.

The hydrogenation and retro-aldol condensation reactions could be conducted on the Cu sites. Therefore, more Cu active sites could promote the hydrogenation and retro-aldol condensation reactions.

The CO-DRIFTS suggested that CuO cannot be completely reduced on the Cu/SiO_2, Cu/ZrO_2 and Cu/TiO_2 catalysts, with some oxidized $Cu^{\delta+}$ species existing. As suggested by the Py-FTIR spectra, only Lewis acid sites existed on the catalyst surface. Therefore, the $Cu^{\delta+}$ species may also act as Lewis acid sites on the catalysts and promote the isomerization, retro-aldol condensation, and the dehydration reactions.[31,69,70]

4. Conclusion

View Article Online
DOI: 10.1039/C8NJ05815F

The synergistic effect between transition metal and metal oxides on the hydrogenolysis of glucose was studied. The product selectivities were strongly influenced by the coordination of hydrogenation metal sites and acid/basic sites. The neutral Cu/SiO_2 catalyst could mainly promote the hydrogenation of glucose. The metal oxides with acid and basic sites could promote the oligomerization reactions of glucose and the unsaturated intermediates without hydrogenation sites. The coordination of high dispersed copper sites and the large amounts of weak and middle Lewis acid sites could tune the isomerization, retro-aldol condensation, and hydrogenation reactions rates, resulting the main product of C_3 polyols. The synergy between the high dispersed copper sites with basic sites could accelerate retro-aldol condensation and isomerization reactions rates simultaneously, resulting the main products of C_2, C_3, and C_4 polyols.

The direct hydrogenolysis of transition metals could also affects the product selectivity. Pd has high selectivity for the central C-C bond cleavage of glucose. However, Ru and Ni have excess hydrogenolysis activity for the terminal of the carbon chain of glucose, with 84.6% alkane selectivity on $Ru/\gamma\text{-}Al_2O_3$.

Glucose and Fructose, with the unsaturated C=O bond, has higher C-C/C-O cleavage activity than the saturated polyols (such as sorbitol and glycerol) in hydrogenation condition. Furthermore, this paper provides a design method of catalyst for the efficient conversion of the saccharides and polyols.

Acknowledgement

This work was financially supported by the Major State Basic Research Development Program of China (973 Program) (No. 2012CB215305), the Natural

Science Foundation of Tianjin (No. 18JCQNJC06600) and the Science & Technology Development Fund of Tianjin Education Commission for Higher Education (No. 2018KJ203). This work was also supported by Synfuels China Co., Ltd.

References

1 A. M. Ruppert, K. Weinberg, R. Palkovits, *Angew. Chem. Int. Ed*., 2012, **51**, 2564-2601.

2 J. N.Chheda, G. W. Huber, J. A. Dumesic, *Angew. Chem. Int. Ed.*, 2007, **46**, 7164-7183.

3 Y. Zheng, X. Chen, Y. Shen, *Chem. Rev*., 2008, **108**, 5253-5277.

4 D. M. Alonso, S. G. Wettstein, J. A. Dumesic, *Chem. Soc. Rev*., 2012, **41**, 8075-8098.

5 M. Patel, A. Kumar, *Renew. Sust. Energ. Rev.*, 2016, **58**, 1293-1307.

6 A. Yepez, A. Pineda, A. Garcia, A. A. Romero, R. Luque, *Phys. Chem. Chem. Phys*., 2013, **15**, 12165-12172.

7 P. Gallezot, N. Nicolaus, G. Flèche, P. Fuertes, A. Perrard, *J. Catal*., 1998, **180**, 51-55.

8 H. Li, W. Wang, J. Deng, *J. Catal*., 2000, **191**, 257-260.

9 G. Zhao, M. Zheng, J. Zhang, A. Wang, T. Zhang, *Ind. Eng. Chem. Res*., 2013, **52**, 9566-9572.

10 W. R. Gunther, Y. Wang, Y. Ji, V. K. Michaelis, S. T. Hunt, R. G. Griffin, Y. Román-Leshkov, *Nature Commun*., 2012, **3**: 1109, 1-8.

11 C. Baatz, U. Prüße, *J. Catal*., 2007, **249**, 34-40.

12 H. Liu, Z. Huang, H. Kang, X. Li, C. Xia, J. Chen, H. Liu, *Appl. Catal. B: Environ*., 2018, **220**, 251-263.

13 N. Li, G. A. Tompsett, T. Zhang, J. Shi, C. E. Wyman, G. W. Huber, *Green Chem*., 2011, **13**, 91-101.

14 G. W. Huber, R. D. Cortright, J. A. Dumesic, *Angew. Chem*., 2004, **116**, 1575-1577.

15 C. W. Lenth, R. N. Du Puis, British Patent, 1939, 499,417.

16 C. W. Lenth, R. N. Du Puis, U. S. Patent, 1940, 2,201,235.

17 Z. Huang, F. Cui, J. Xue ,J. Zuo, J. Chen ,C. Xia *Catal. Today*, 2012, **183**, 42-51.

18 B. Blanc, A. Bourrel, P. Gallezot, T. Haas, P. Taylor, *Green Chem*., 2000, **2**, 89-91.

19 W. H. Zartman, H. Adkins, *J. Am. Chem. Soc*., 1933, **55**, 4559-4563.

20 L. Guo, J. Zhou, J. Mao, X. Guo, S. Zhang, *Appl. Catal. A-Gen*., 2009, **367**, 93-98.

21 I. Gandarias, P. L. Arias, J. Requies, M. E. Doukkali, M. B. Güemez, *J. Catal.*, 2011, **282**, 237-247.

22 J. Chaminand, L. Djakovitch, P. Gallezot, P. Marion, C. Pinel, C. Rosier, *Green Chem*., 2004, **6**, 359-361.

23 M. A. Andrews, S. A. Klaeren, *J. Am. Chem. Soc*., 1989, **111**, 4131-4133.

24 J. Sun, H. Liu, *Green Chem*., 2011, **13**, 135-142.

25 X. Chen, X. Wang, S. Yao, X. Mu, *Catal. Commun*., 2013, **39**, 86-89.

26 Y. T. Kim, J. A. Dumesic, G. W. Huber, *J. Catal*., 2013, **304**, 72-85.

27. X. Wang, X. Liu, Y. Xu, G. Peng, Q. Cao, X. Mu, Chinese *J. Catal*., 2015, **36**, 1614-1622.

28. Z. Huang, J. Chen, Y. Jia, H. Liu, C. Xia, H. Liu, *Appl. Catal. B: Environ*., 2014, **147**, 377-386.

39 G. C. Bond, S. N. Namijo, *J. Catal*., 1989, **118**, 507-510.

30 C. J. G. Van Der Grift, A. F. H. Wielers, B. P. J. Jogh, J. Van Beunum, M. De Boer, M. Versluijs-Helder, W. Geus, *J. Catal.*, 1991, **131**, 178-189.

31 B. Zhang, Y. Zhu, G. Ding, H. Zheng, Y. Li, *Appl. Catal. A-Gen.*, 2012, **443-444**, 191-201.

32 S. Zhu, Y. Zhu, S. Hao, H. Zheng, T. Mo, Y. Li, *Green Chem.*, 2012, **14**, 2607-2616.

33 M. Watanabe, Y. Aizawa, ToruIida, R. Nishimura, H. Inomata. *Appl. Catal. A-Gen.*, 2005, **295**, 150-156.

34 S. Zhu, X. Gao, Y. Zhu, Y. Zhu, H. Zheng, Y. Li, *J. Catal*., 2013, **303**, 70-79.

35 E. P. Maris, W. C. Ketchie, V. Oleshko, R. J. Davis, *J. Phys. Chem. B*, 2006, **110**, 7869-7876.

36 C. Gu, G. Li, Y. Hu, S. Qing, X. Hou, Z. Gao, *J. Fuel Chem. Technol*., 2012, **40 (11)**, 1328-1335.

37 Z. Yan, H. Yang, J. Ouyang, A. Tang， *Chem. Eng. J*., 2017, **316**, 1035-1046.

38 A. Dandekar, M. A. Vannice, *J. Catal*., 1998, **178**, 621-639.

39 C. S. Chen, J. H. You, J. H. Lin, Y. Y. Chen, *Catal. Commun*., 2008, **9**, 2381-2385.

40 F. Boccuzzi, A. Chiorino, G. Martra, M. Gargano, N. Ravasio, B. Carrozzini, *J. Catal*., 1997, **165**, 129-139.

41 R. M. Ferullo. N. J. Castellani, *J. Mol. Catal. A-Chem*., 2005, **234**, 121-127.

42 C. Morterra, E. Giamello, G. Cerrato, G. Centi, and S. Per ,athoner, *J. Catal*., 1998, **179**, 111-

View Article Online
DOI: 10.1039/C8NJ05815F

128.

43 T. Venkov, M. Dimitrov, K. Hadjiivanov, *J. Mol. Catal. A-Chem.*, 2006, **243**, 8-16.

44 M. Mihet, M. D. Lazar, *Catal. Today*, 2018, **306**, 294-299.

45 Ahmed Al-Fatesh, *JKSUES*, 2015, **27**, 101-107.

46 M. Nagai, K. Koizumi, S. Omi, *Catal. Today*, 1997, **35**, 393-405.

47 V. S. Kumar, B. M. Nagaraja, V. Shashikala, P. Seetharamulu, A. H. Padmasri, B. D. Raju, K. S. R. Rao, *J. Mol. Catal. A-Chem.*, 2004, **223**, 283-288.

48 E. P. Parry, *J. Catal*., 1963, **2**, 371-379.

49 M. I. ZaKi, M. A. Hasan, F. A. Al-Sagheer, L. Pasupulety, *Colloid. Surface. A*, 2001, **190**, 261-274.

50 P. Concepción, M. T. Navarro, T. Blasco, J. M. López Nieto, B. Panzacchi, F. Rey, *Catal. Today*, 2004, 96, 179-186.

51 X. Chen, G. Clet, K. Thomas, M. Houalla, *J. Catal.*, 2010, **273**, 236-244.

52 N. Li, G. W. Huber, *J. Catal*., 2010, **270**, 48-59.

53 P. A. Torresi, V. K. Díez, P. J. Luggren, J. I. Di Cosimo, *Appl. Catal. A: Gen*., 2013, **458**, 119-129.

54 C. Montassier, J. C. Ménézo, L. C. Hoang, C. Renaud, J. Barbier, *J. Mol. Catal.*, 1991, **70**, 99-110.

55 D. K. Sohounloue, C. Montassier, J. Barbier, *React. Kinet. Catal. Lett*., 1983, **29**, 391-397.

56 K. Wang, M. C. Hawley, T. D. Furney, *Ind. Eng. Chem. Res*., 1995, **34**, 3766-3770.

57 P. A. Lazaridis, S. Karakoulia, A. Delimitis, S. M. Coman, V. I. Parvulescu, K. S. Triantafyllidis, *Catal. Today*, 2015, **257**, 281-290.

58 L. Ye, X. Duan, H. Lin, Y. Yuan, *Catal. Today*, 2012, **183**, 65-71.

59 C. Liu, C. Zhang, K. Liu, Y. Wang, G. Fan, S. Sun, J. Xu, Y. Zhu, Y. Li, *Biomass & Bioenergy*, 2015, **72**, 189-199.

60 M. Sasaki, K. Goto, K. Tajima, T. Adschiri and K. Arai, *Green Chem*., 2002, **4**, 285-287.

61 C. J. Barrett, J. N. Chheda, G. W. Huber, J. A. Dumesic, *Appl. Catal. B-Environ.*, 2006, **66**, 111-118.

62 G. W. Huber, J. N. Chheda, C. J. Barrett, J. A. Dumesic, *Science*, 2005, **308**, 1446-1450.

63 C. Liu, C. Zhang, S. Hao, S. Sun, K. Liu, J. Xu, Y. Zhu, Y. Li, *Catal. Today*, 2016, **261**, 116-127.

64 Y. Kanie, K. Akiyama, M. Iwamoto, *Catal. Today*, 2011, **178**, 58-63.

65 P. Ooms, M. Dusselier, J. A. Geboers, B. O. Beeck, R. Verhaeven, E. Gobechiya, J. A. Martens, A. Redl, B. F. Sels, *Green Chem*., 2014, **16**, 695-707.

66 Y. Liu, Y. Liu, Y. Zhang, *Appl. Catal. B: Environ*., 2019, **242**, 100-108.

67 J. Pang, M. Zheng, X. Li, Y. Jiang, Y. Zhao, A. Wang, J. Wang, X. Wang, T. Zhang, *Appl. Catal. B: Environ*., 2018, **239**, 300-308.

68 M. S. Holm, S. Saravanamurugan, E. Taarning, *Science*, 2010, **328**, 602-605.

69 A. Yin, X. Guo, W. L. Dai, K. Fan, *J. Phys. Chem. C*, 2009, **113**, 11003-11013.

70 B. Z. Sun, W. K. Chen, X. Wang, C. H. Lu, *Appl. Surf. Sci*., 2007, **253**, 7501-7505.

View Article Online
DOI: 10.1039/C8NJ05815F

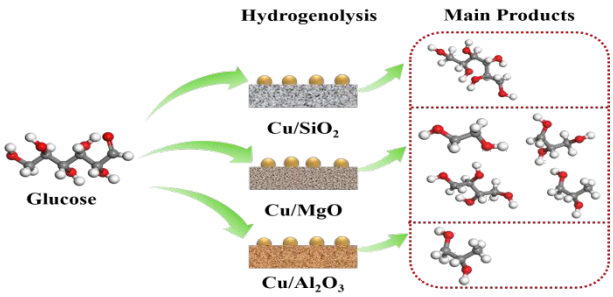

The coordination of copper and different acid/basic sites could promote the selective hydrogenolysis of glucose to polyols.